Research Report

Modeling of Diesel Spray Atomization Linked with Internal Nozzle Flow

Makoto Nagaoka, Reiko Ueda, Ryo Masuda, Eberhard von Berg and Reinhard Tatschl

Report received on Mar. 18, 2011

ABSTRACT A computational fluid dynamics (CFD) model is enhanced to predict Diesel spray characteristics without any specific experimental spray data. A series CFD calculation methodology from injector nozzle internal flow to fuel spray in a chamber is applied. The calculated spray characteristics, which are spray shape, tip penetration, angle and droplet size distributions of both mini-sac (MS) and valve covered orifice (VCO) nozzles in a constant volume vessel are compared with the measurement data and quantitatively reproduced. The calculation results show the relations between nozzle geometry and spray characteristics, such as effect of nozzle length-diameter ratio on cavitation suppression or asymmetric nature of spray shape of VCO nozzle.

KEYWORDS Diesel engine, Computational fluid dynamics, Spray, Atomization, Internal nozzle flow

Notation

a,b	*Radii of main axis of a spheroid, which is rotational symmetric on the b-axis..*
a_p	*Droplet acceleration.*
B_0,B_1	*Constants of Kelvin-Helmholtz breakup model.*
C_0,C_1	*Constants of Rayleigh-Taylor breakup model.*
C_D	*Drag coefficient.*
D	*Nozzle exit diameter.*
L	*Nozzle hole length.*
R	*Nozzle inlet curvature radius.*
r	*Radius of droplet or sphere.*
r_0	*Equivalent spherical radius of spheroidal droplet.*
SMD	*Sauter Mean Diameter.*
t	*Time.*
U	*Relative velocity between droplet and gas.*
Y	*Droplet deformation ratio, $Y=a/r_0$.*
Λ	*Wave length of fastest instability wave.*
μ	*Viscous coefficient.*
θ	*Angle.*
ρ	*Density.*
σ	*Surface tension coefficient.*
τ	*Breakup time scale.*
Ω	*Growth rate of fastest instabilty wave.*

Subscripts

d	*Droplet.*
g	*Gas.*
KH	*Kelvin-Helmholtz breakup model.*
l	*Liquid.*
RT	*Rayleigh-Taylor breakup model.*
st	*Stable droplet.*

1. Introduction

Fuel injector characteristic features directly affect the performance of a direct injection Diesel engine. Spray characteristics are defined by the internal nozzle flow as well as the ambient gas field. Many of recent works for spray characterization are linked with internal nozzle flow, which is more important at the nozzle exit as upstream boundary condition of spray.[1-4] No general solutions for spray and combustion in an engine cylinder are obtained without taking into account the injector nozzle flow distribution. The flow in a nozzle is transient and has highly three-dimensional distribution so that three-dimensional computational fluid dynamics (CFD) is necessary for the numerical analysis. The authors[5,6] have also proposed a series calculation methodology linking the three-dimensional Eulerian multiphase nozzle internal flow calculation with the Eulerian-Lagrangian spray calculation. In this method, the spatial distributions of physical quantities at the nozzle hole exit are inherited by the primary break-up model. The break-up mechanism is modeled taking into account the injection jet, cavitation and turbulence. Through the succeeding secondary breakup model, the spray characteristics are simulated. However, the application to many injector nozzle dimensional data leads to high

effort for model parameter adjustment.

The objective of this work is to establish a CFD method to predict Diesel spray characteristics without any specific experimental spray data and model parameter adjustment for standard injector nozzle geometry. The calculations from an injector nozzle internal flow to spray formation in a constant volume vessel are performed for typical Diesel nozzles, that is mini-sac (MS) and valve covered orifice (VCO) nozzles, in recent common rail injector system. The validation of the calculation results is done by comparison with the measurement data. From the analysis of calculation results, an important relation between the nozzle geometry and spray characteristics becomes clear.

2. Calculation Method

2. 1 Calculation models

2. 1. 1 Nozzle internal flow

An Eulerian three-fluid model with a cavitation model[7] in the CFD code AVL FIRE is used to calculate cavitating flow in a nozzle. Three fluids are composed of diesel fuel liquid, diesel fuel vapor and ambient gas. The ensemble averaged transport equations for mass, momentum, turbulence kinetic energy and its dissipation rate are solved separately for each phase. The governing equations for each phase are characterized by the volume fraction and additional inter-phase exchange terms, which account for the two-phase interaction.

2. 1. 2 Breakup model

The transient data of spatial distributions of flow velocity, void fraction, turbulent kinetic energy and its dissipation rate at the nozzle hole exit are extracted from the internal nozzle flow calculations and transferred to a primary break-up model as the boundary conditions of spray calculations.[6] The primary break-up model, that is Diesel breakup model in the FIRE code, is based on simulating the competing effects of aerodynamic, turbulence and cavitation induced breakup processes. However, the different model constants from the defaults are obtained in the validation step. And it has been difficult to simulate the droplet size distributions as well as other spray characteristics only by the conventional model constant adjustment. A novel secondary breakup model with droplet deformation drag, which is a variant of the Kelvin-Helmholtz and Rayleigh-Taylor instability (KH-RT) model,[8] has been developed and incorporated in the FIRE. The model is based on the one developed for direct injection gasoline engines.[9] The feature is modeling break-up process due to dynamic droplet deformation. The drop shape deformed by ambient gas drag force is assumed to be a rotational spheroid. The nonlinear model equation is theoretically conducted from the energy conservation in a liquid drop. It is a little bit inconvenient on practical use because it is solved by numerical integration and requires small time increment. The following equation linearised at the equilibrium point, $Y = 1$, is used herein, that is actually the same as the TAB model.[10]

$$\ddot{Y} + 10N\dot{Y} + 8K(Y-1) = \frac{1}{6}KWe_g \quad \cdots\cdots\cdots (1)$$

$$Y = \frac{a}{r_0},\ K = \frac{\sigma}{\rho_d r_0^3},\ N = \frac{\mu_d}{\rho_d r_0^2},\ We_g = \frac{\rho_g U^2 2r_0}{\sigma}$$

The drag coefficient C_D is given as the following:

$$C_D = \min\left[C_{D,disk}, C_{D,sphere}\left(0.932\,a/b + 0.034\,b/a + 0.034\sqrt{a/b}\right)\right] \quad \cdots (2)$$

$C_{D,\,disk} = 1.12$, $C_{D,\,sphere} = 0.424$

The Eq. 2 is applicable to higher droplet Reynolds number in which the pressure drag is dominant and the coefficient is less dependent on the Reynolds number. In lower Reynolds number, the drag increases due to the skin friction. The coefficient in the lower Reynolds number is given by that of a sphere.

$$C_D = \frac{24}{\mathrm{Re}_d}\left(1 + \frac{1}{6}\mathrm{Re}_d^{2/3}\right) \quad \cdots\cdots\cdots\cdots\cdots (3)$$

The KH-RT model for secondary breakup is modified in this study. The KH model equation is the same except for using spheroid radius instead of sphere one.

$$\frac{da}{dt} = -\frac{a - r_{st}}{\tau_{KH}} \quad \cdots\cdots\cdots\cdots\cdots\cdots\cdots (4)$$

$$r_{st} = B_0 \Lambda_{KH} \quad \cdots\cdots\cdots\cdots\cdots\cdots\cdots\cdots (5)$$

$$\tau_{KH} = 3.7B_1 a/\Lambda_{KH}\Omega_{KH} \cdots\cdots\cdots\cdots\cdots (6)$$

The circumference of spheroidal droplet is stripped by gas shear flow so that the spheroidal symmetric axis radius b is kept and only the other radius a decreases. The deformation ratio is also corrected.

The breakup criterion in the R-T model is given by the following equation.

$$\int_0^{t_b} \frac{dt}{\tau_{RT}} = 1 \cdots\cdots\cdots\cdots\cdots\cdots\cdots (7)$$

$$1/\tau_{RT} = C_1\Omega_{RT} = C_1\sqrt{\frac{2}{3}\frac{\rho_\ell - \rho_g}{\rho_\ell + \rho_g}a_p}\frac{2\pi}{\Lambda_{RT}} \cdots (8)$$

$$\Lambda_{RT} = 2\pi\sqrt{\frac{3\sigma}{(\rho_\ell - \rho_g)a_p}} \cdots\cdots\cdots\cdots (9)$$

The droplet acceleration a_p is calculated using the above mentioned spheroid drag coefficient. In the Eq. 7, the breakup time elapses only when droplet diameter is larger than the characteristic length scale.

$$r_{RT} = C_0\Lambda_{RT} \cdots\cdots\cdots\cdots\cdots\cdots\cdots (10)$$

where B_0 = 0.61, B_1 = 35, C_0 = 5.3, C_1 = 1. In our model, KH and RT models are parallel progresses.

There are some differences from the original WAVE model[11] in the child drop shedding.

(1) Only one child drop is shed from one parcel. That means the grandchild drop shedding is prohibited in order to avoid excessive number of small drops.
(2) When the accumulated parcel mass, not droplet mass, of liquid to be removed from the parent reaches or exceeds a half of initial parcel mass, the child droplet is produced and the parcel mass is 15% of the accumulated one. This constant is derived from experimental database of droplet size distribution, in which some are used in the present calculation validation.
(3) The child drop size is not the single stable one given by the Eq. 5, but stochastically given according to chi-square distribution with degrees of freedom eight. The stable radius is treated as the SMD.
(4) The velocity component normal to parent droplet velocity vector is also stochastically multiplied with a factor of random number from zero to one.

2. 2 Calculation procedure

Three steps are taken in our spray simulation linked with nozzle internal flow. The first step is steady flow calculation with full needle lift and specified pressure drop for the nozzle flow rate test rig. The objective is to specify the nozzle hole inlet roundness figured by hydro-grinding. The discharge coefficient is compared with the design value or experimental one, and the roundness is corrected until coinciding. Eventually, the computational mesh with some nozzle inlet roundness is obtained and employed for the following calculation. The second step is transient calculation of nozzle internal flow with needle movement. This is performed to simulate the actual operating condition. The needle lift curve is given by the lift sensor output in the present study. But one-dimensional injection system simulation is also available to give the lift curve and upstream boundary conditions. Eventually, the transient data of nozzle exit flow variables is obtained and used as boundary conditions in the succeeding spray simulation as the third step.

The spray model is based on the discrete droplet model (DDM). The linear weight interpolation for gas flow velocity is used in the droplet-gas relative velocity. This effect on spray tip penetration is considerable. The droplet interaction model [12,13] is also used.

2. 3 Nozzle geometry and test conditions

The typical computational meshes for the MS and VCO nozzles are shown in **Fig. 1**. Due to the symmetrical injector geometry, the mesh is one sector for a single nozzle hole. The nozzle is attached to

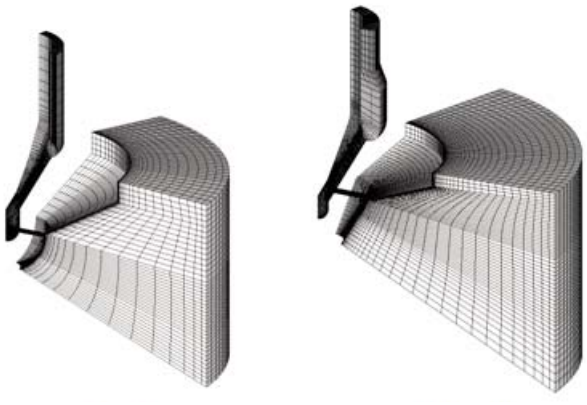

MS nozzle VCO nozzle

Fig. 1 Computational grids for MS and VCO nozzles.

common rail injector system. The double-guided VCO nozzle is employed to minimize the variation of sprays from the nozzle holes. The configuration of nozzles and calculation conditions of injection operation are shown in **Table 1**. For each nozzle type, the number of nozzle hole is modified according to the diameter in order to keep the same range of total mass flow rate. Therefore, the nozzles with diameter 0.18 of which the number of hole and diameter are far from the specification of current HSDI Diesel engine injectors are evaluated just for comparisons.

The calculations are validated for spray injected in a constant volume vessel. The fuel pressure is 87.5 MPa. The ambient gas is CO_2 and its pressure is 2.1MPa, corresponding to a gas density of 38.6 kg/m^3. The pressure boundary condition at the nozzle upstream is set to be constant. Some volume is added outside of the nozzle, and the outer boundary condition is set to be a constant back pressure. The roundness R at the nozzle hole inlet is set to be 10% of nozzle diameter for all nozzles except for the MS nozzle with D = 0.10 mm and L = 0.8mm, of which R/D is 20%. Those give good agreement with measured discharge coefficient within 5% deviation. The discharge coefficients obtained by the CFD calculation are also shown in Table 1 while the designed values are 0.81 for the MS nozzles and 0.74 for the VCO nozzles, respectively. **Figure 2** shows needle lift profile. The needle lift profiles of all nozzles are similar because the same injector is used. The trapezoidal shape is approximated for calculations, and each instant of time is shown in Table 1. Since the solver does not handle the mesh whose size is zero, the initial needle lift is set to 10 micron. The meshes of the clearance between the needle and nozzle body stretch and shrink according to the needle displacement.

3. Results and discussions

3. 1 Nozzle internal flow

The comparisons of injection volume flow rate are shown in **Fig. 3**. The measurement was done using an injection rate meter based on Zeuch method. The calculation results agree well quantitatively with the measurement except for a little overestimation in the initial lift-up period. One reason is that the initial needle lift is set at 10 micron in the calculation. Another one would be the difference of the ambience outside of a nozzle. The back pressure is the same between the calculation and experiment, but it is filled with fuel liquid in the measurements while CO_2 gas in the calculations as the spray experiment. Nonetheless, they coincide within 5% of difference on the total injection volumes. **Figure 4** shows liquid volume fraction in the nozzle hole at full lift timing. As known well, the VCO nozzle enhances cavitation generation at the nozzle hole inlet which usually causes lower

Table 1 Test nozzle specifications and conditions (* Calculated).

Nozzle	n	D(mm)	L(mm)	R/D	Cd*	T1 (ms)	T2 (ms)	T3 (ms)
MS	9	0.10	0.8	0.2	0.80	1.0	1.24	2.0
MS	5	0.14	0.8	0.1	0.81	1.0	1.24	2.0
MS	3	0.18	0.8	0.1	0.81	1.0	1.24	2.0
MS	5	0.14	0.6	0.1	0.82	1.04	1.32	2.0
MS	5	0.14	1.0	0.1	0.80	1.04	1.32	2.04
VCO	9	0.10	1.0	0.1	0.74	0.99	1.17	1.96
VCO	5	0.14	1.0	0.1	0.75	1.0	1.19	1.98
VCO	3	0.18	1.0	0.1	0.74	0.96	1.18	1.96

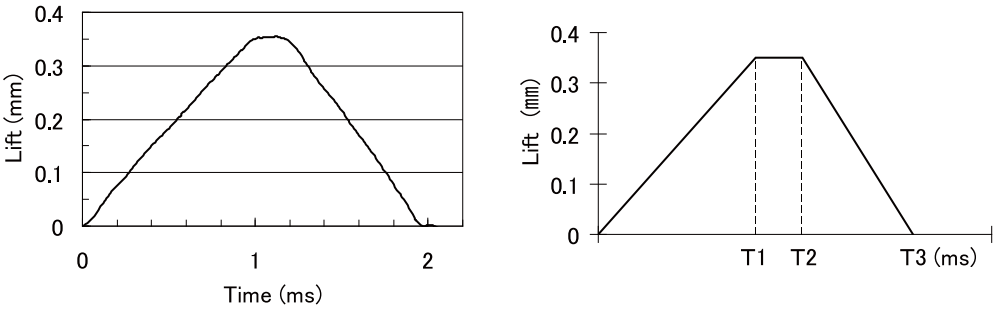

Fig. 2 Needle lift profile (Left; measured one for VCO (D = 0.14) nozzle, Right; approximated for calculations).

discharge coefficient of a VCO nozzle than a MS nozzle. It is also shown that the cavitation in nozzle hole exit is suppressed by smaller hole diameter or larger hole length regardless of nozzle type. The linear correlation between cavitation volume at the nozzle exit and the nozzle L/D is predicted in the calculations as shown in **Fig. 5**. The lower L/D brings in more enhanced cavitating flow injection, which could produce finer atomization and lower penetration spray.

3. 2 Spray formation

3 .2. 1 Spray validation

The experiments for spray calculation validation have been done on an optically accessible high pressure cold constant volume vessel. The scattered light images reflected from spray droplet are captured with a single shot laser pulse light source and a high resolution CCD camera. The Dantec PDA system for high density spray has been used to measure droplet size. The measurement point is on the spray axis and the spray tip at 3.6 ms after injection, which is around 60 to 80 mm from the nozzle exit. The measurement period is from the start of injection to 8 ms by which almost all spray main stream passes. To compare droplet size between calculation and measurement, the calculated spray parcels are sampled passing within 1 mm of the measurement point by the same timing 8 ms. The spray characteristics, those are spray shape,

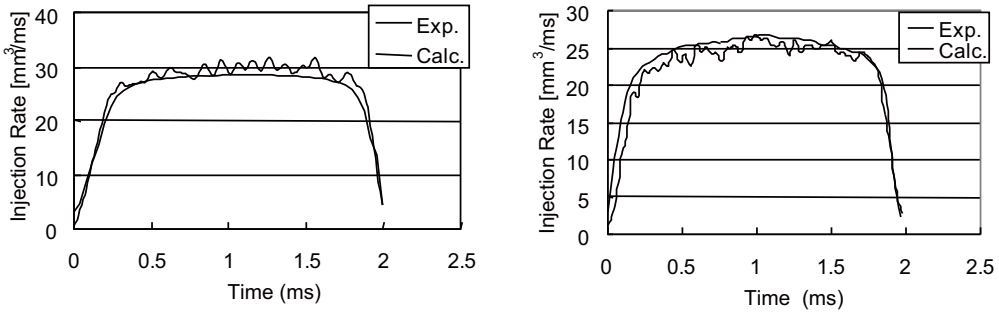

(a) MS nozzle (D=0.14, L=0.8) (b) VCO nozzle (D=0.14, L=1.0)

Fig. 3 Comparisons injection volume flow rate.

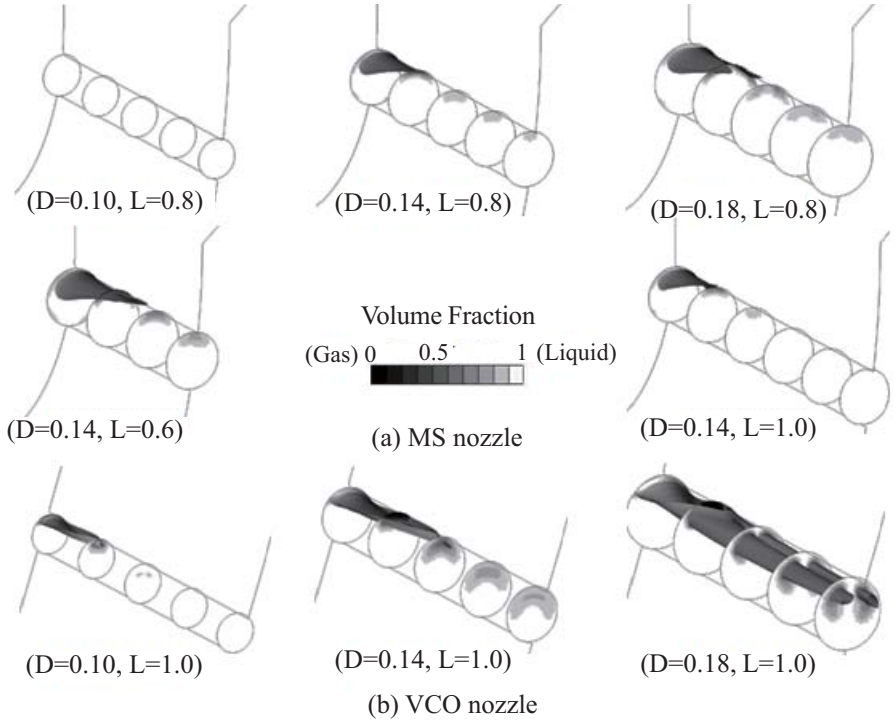

Fig. 4 Liquid volume fraction on the cross section and iso-surface equal to 0.5 (t = 1.0 ms).

tip penetration, spray angle, SMD and droplet size distributions of both volume and number density are compared. The definition of spray angle is shown in **Fig. 6**, the wide angle of a nozzle exit point and two spray width edges at 70% of tip penetration at the end of injection. The measurement spray tip penetration and angle are averaged in those of all nozzle holes.

Spray calculations have been done for the nozzles in previous section except for nozzle diameter 0.18 mm. **Figure 7** shows computational grid of a constant volume vessel. The size near nozzle exit is almost equal to the nozzle diameter and the mesh is fine only in spray region. The calculation results of nozzle internal flow are given at the nozzle exit as the boundary conditions of spray calculation.

A lot of calculation tests have been done for validation with many combinations of primary and secondary breakup model parameters using conventional Diesel primary breakup and WAVE models. **Figure 8** shows one of the calculation results closest to the experimental one. Other calculation results were worse than this. The penetration and SMD were in good agreement, however, the calculated

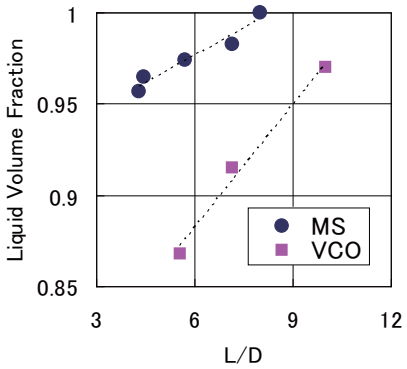

Fig. 5 Liquid volume fraction of nozzle exit at t = 1.0 ms versus nozzle L/D.

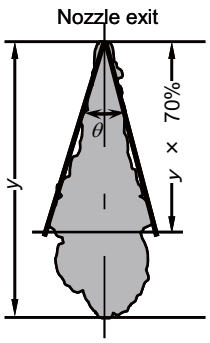

Fig. 6 Definition of spray angle.

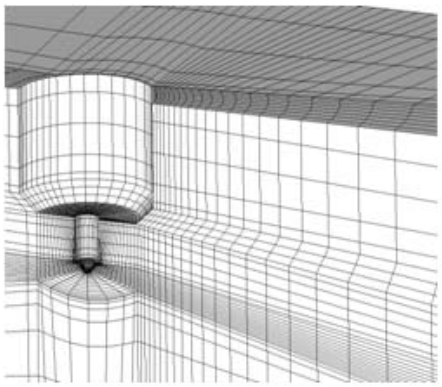

Fig. 7 Computational grid for spray in a constant volume vessel.

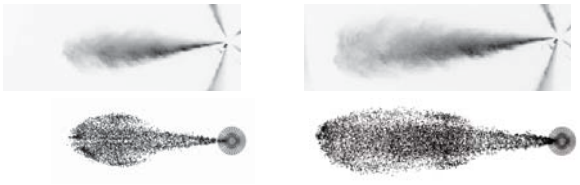

(a) Spray shape (upper: experiment, lower: calculation)

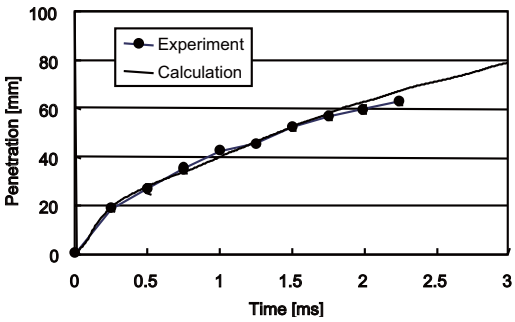

(b) Spray tip penetration

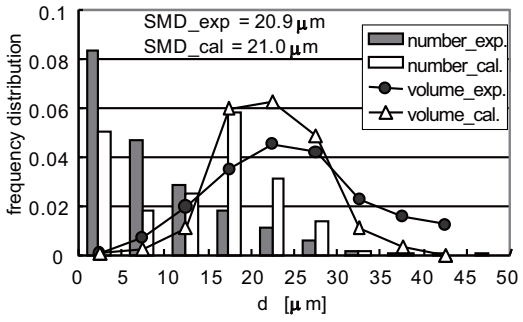

(c) Spray droplet size distributions and SMD

Fig. 8 Comparisons of experiment and calculation using conventional droplet breakup models (MS nozzle, D = 0.14, L = 1.0).

number distribution of droplet size was bi-modal and the spray shape was oval unlike the experiment. Those experiences of model parameter optimization made clear the following things:

- Without child parcel production, number distribution of smaller droplet size cannot be reproduced.
- But, it is too difficult for the conventional models to give wider range of droplet size distribution as in the experiment. Sometimes unrealistic bi-modal size distribution was obtained because of parent drop and child drop size disjunction.
- The secondary breakup model is more effective on spray shape formation and tip penetration, while child parcel shedding is less effective.

The new secondary breakup model as mentioned in the previous chapter is used. **Figure 9** shows comparison of spray shape both for MS and VCO nozzles. The spray tip penetrations and spray angle are shown in **Fig. 10** and **Fig. 11**, respectively. All of them agree well. **Figure 12** shows droplet size distributions and SMD values. There is not so much difference of SMD among the nozzles tested here. The number distribution simply increases with smaller droplet size. These features are quantitatively reproduced well in all the calculations without any model parameter adjustment for each. The new features of size distribution for child parcel diameter and reduced number of child parcels resolve the unrealistic bi-

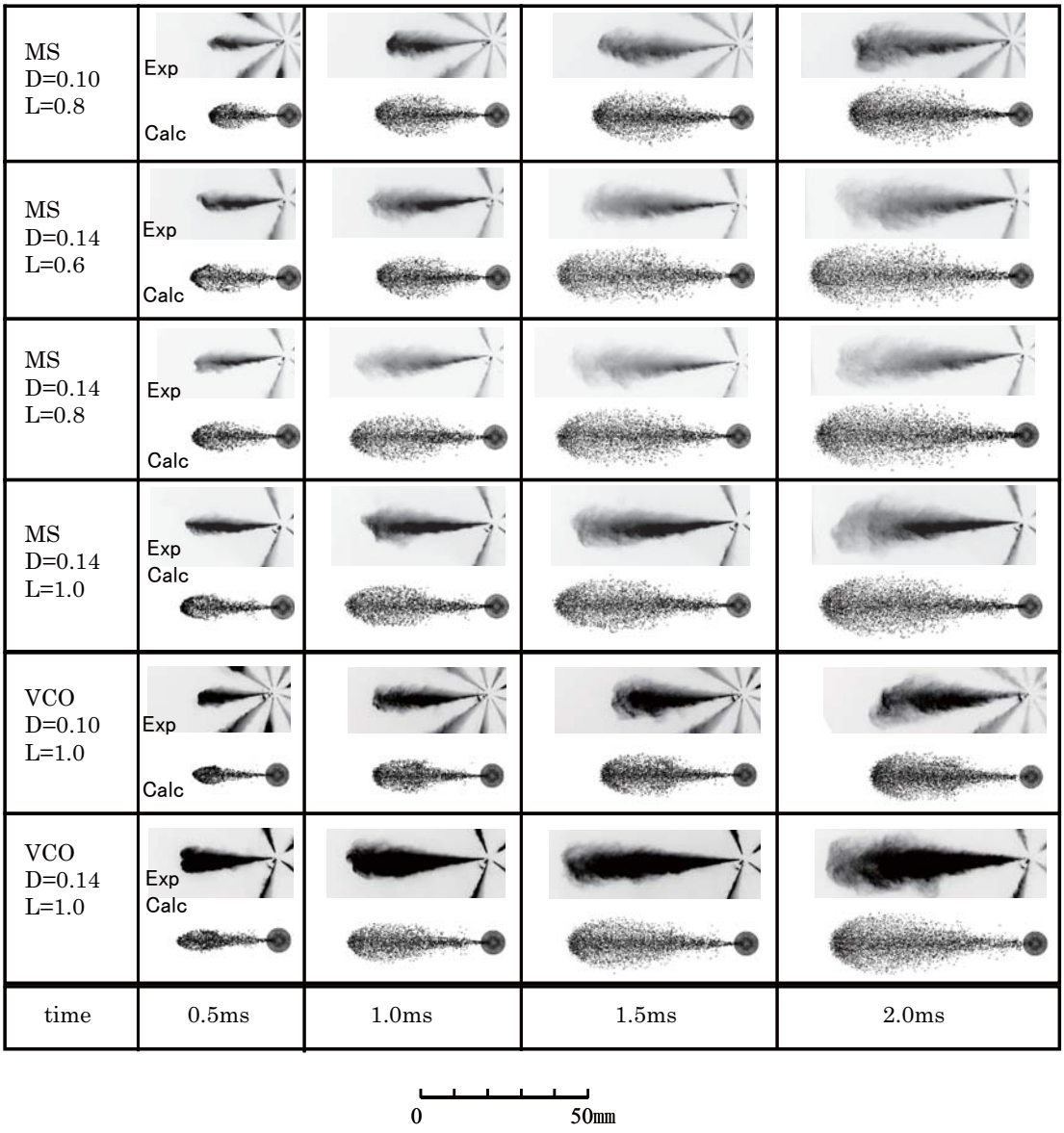

Fig. 9 Comparisons of spray shape between experiment and calculation using present breakup model.

modal distribution. The droplet deformation drag model is also effective to the spray shape improvement, on which it gives spindle-shape like experiment.

3. 2. 2 Analysis of spray shape

Although the bottom-up view of spray as shown in Fig. 9 looks similar between MS and VCO nozzles with the same nozzle diameter, it is found that the side view of spray is different. The calculations have predicted the results, as shown in **Fig. 13,** that the spray shape of MS nozzle is symmetric along the spray axis, while asymmetric of the VCO nozzle. The forefront of spray spreads downside in the VCO nozzle. To confirm this prediction, the side view image was captured using a high-speed camera. Only one spray from a nozzle hole is observed attached with a shield jacket to separate other sprays. As shown in **Fig. 14**, the side view imaging validates the calculation results. We believe that this feature is not special to this nozzle but more or less a general feature of VCO nozzle.

This feature is derived from the flow pattern into a nozzle hole. **Figure 15** shows the flow pattern in the nozzles. In the VCO nozzle, the fuel until 0.1 ms after the needle opening flows into the downside of nozzle orifice inlet so that the velocity of lower half in the nozzle hole is larger. The jet forms a main stream of spray so that the lower half of spray penetration is stronger than upper half. The cavitation does not play an important role in this initial stage. The cavitation reaches the nozzle exit at about 0.1 ms as shown in **Fig. 16** and it pushes this one-sided flow over 0.2 ms again.

The bias decreases with the needle lifting up and nozzle flow development. But the influence of the initial nozzle flow pattern on the spray shape remains over 1 ms. On the liquid mass distributions as shown in **Fig. 17**, though the periphery looks smeared due to grid resolution in the graphical post-processing, the difference of symmetry property is clear between MS and VCO nozzles. The induced gas flow field around

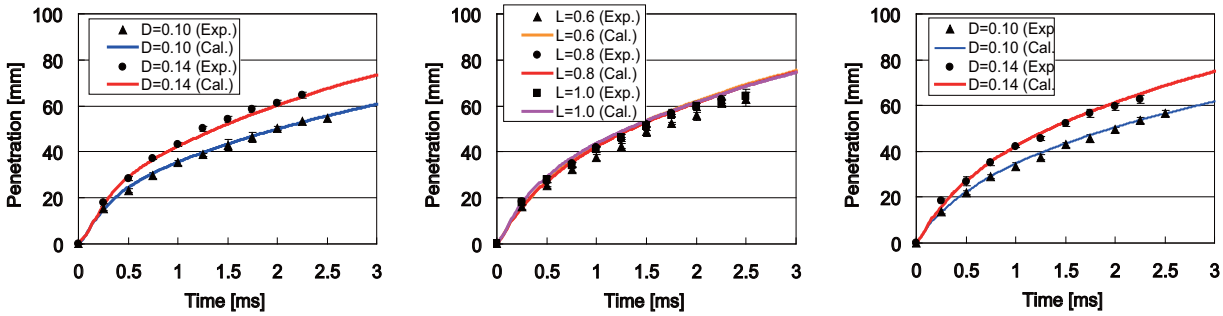

(a) MS nozzle (L=0.8) (b) MS nozzle (D=0.14) (c) VCO nozzle (L=1.0)

Fig. 10 Comparisons of spray tip penetration between experiment and calculation using present breakup model.

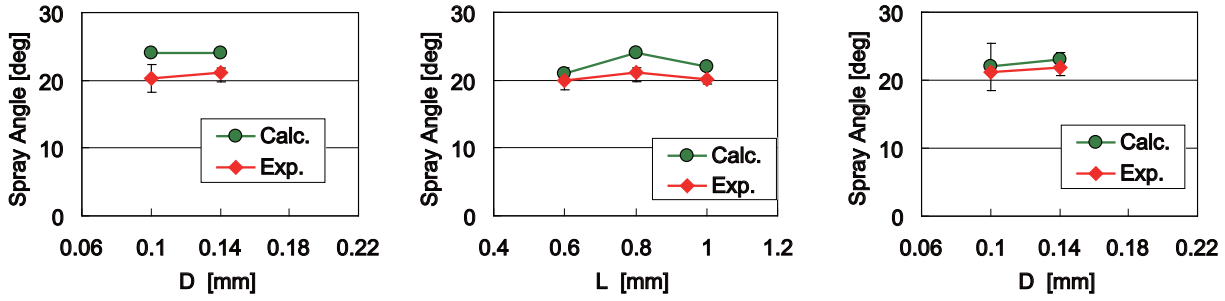

(a) MS nozzle (L=0.8) (b) MS nozzle (D=0.14) (c) VCO nozzle (L=1.0)

Fig. 11 Comparisons of spray angle between experiment and calculation using present breakup model.

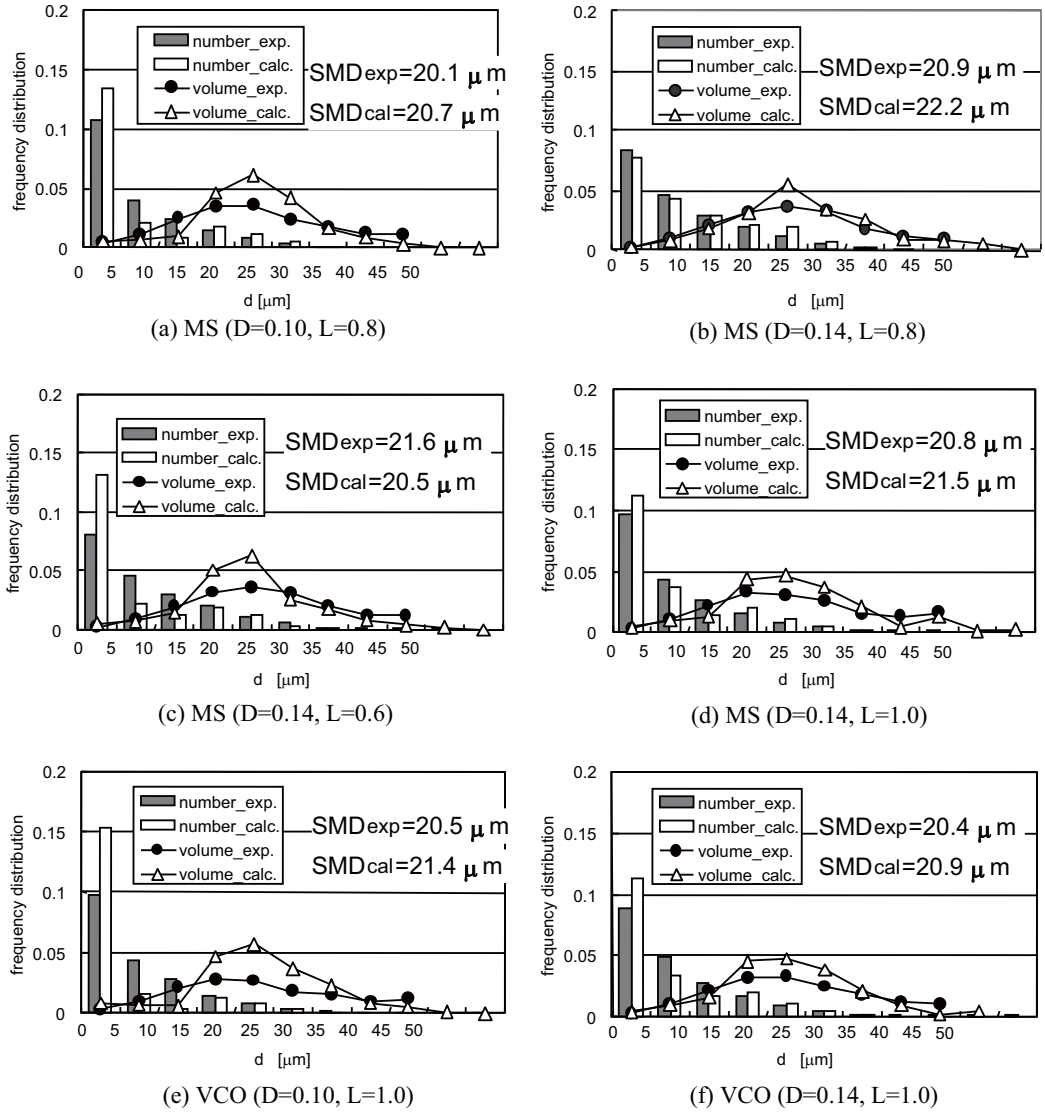

(a) MS (D=0.10, L=0.8)
(b) MS (D=0.14, L=0.8)
(c) MS (D=0.14, L=0.6)
(d) MS (D=0.14, L=1.0)
(e) VCO (D=0.10, L=1.0)
(f) VCO (D=0.14, L=1.0)

Fig. 12 Comparison of spray size distributions and SMD between experiment and calculation using present breakup model (line, droplet number; symbol, volume; black, experiment; white, calculation).

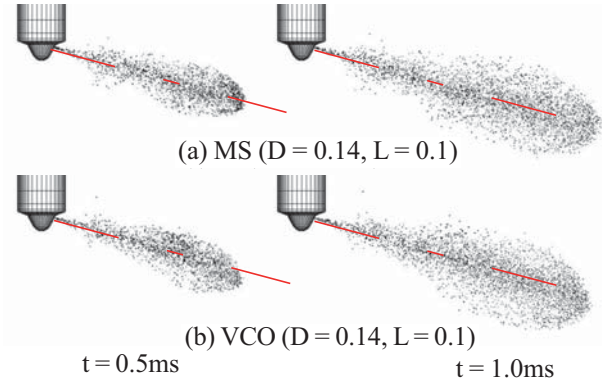

(a) MS (D = 0.14, L = 0.1)
(b) VCO (D = 0.14, L = 0.1)
t = 0.5ms
t = 1.0ms

Fig. 13 Side view calculated spray parcel plot with spray axis.

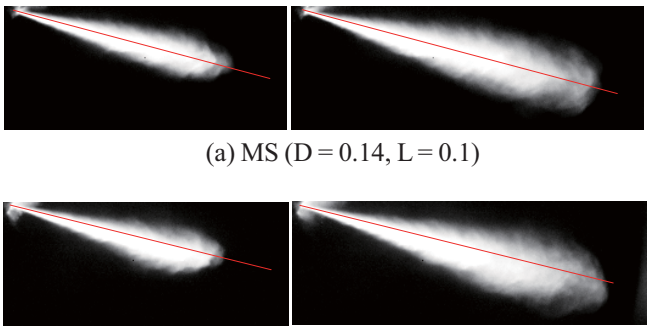

(a) MS (D = 0.14, L = 0.1)
(b) VCO (D = 0.14, L = 0.1)
t = 0.5ms
t = 1.0ms

Fig. 14 Side view experimental spray image with spray axis (Fuel pressure 90 MPa, Ambient gas, CO_2 pressure 1.1 MPa).

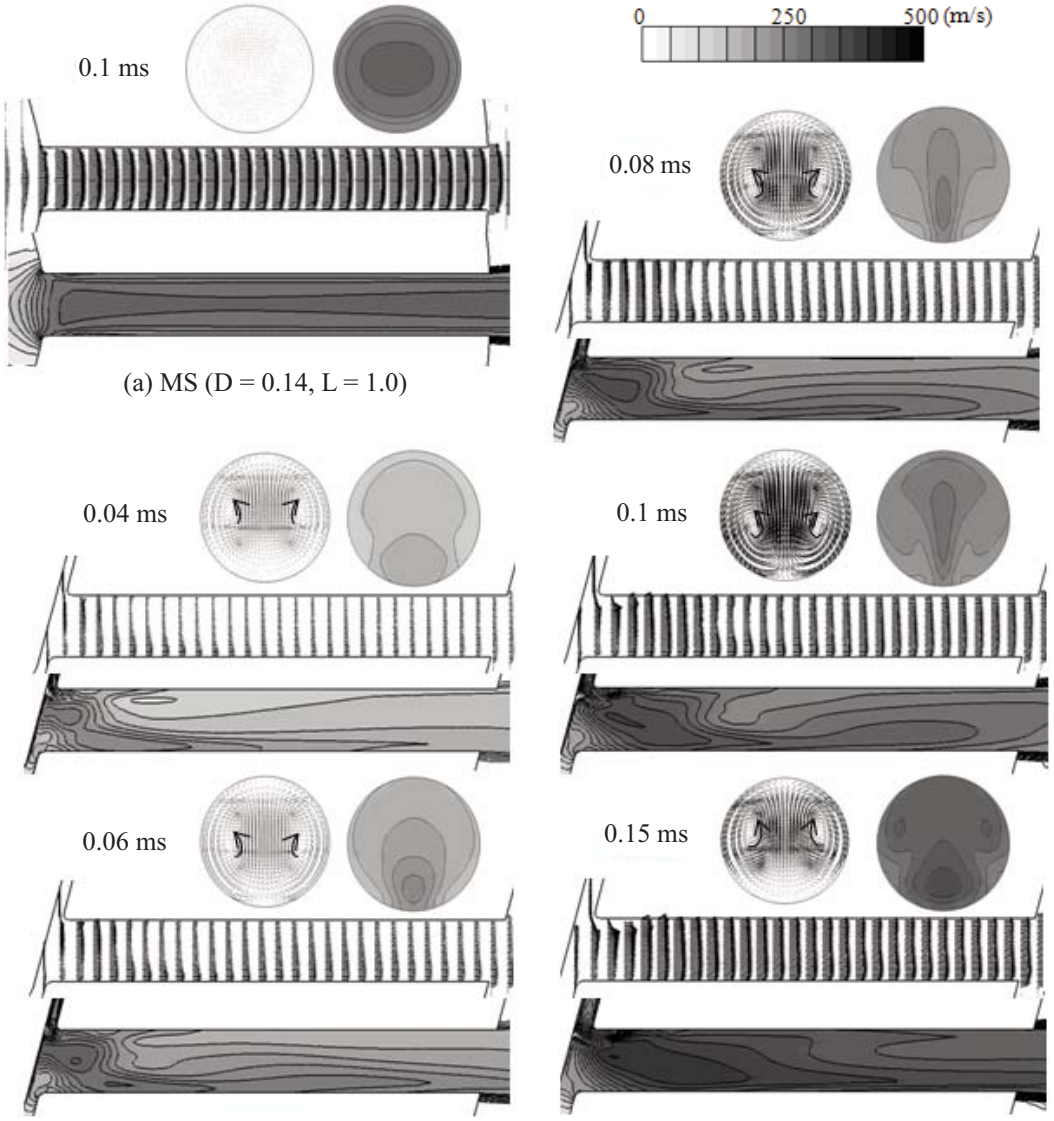

Fig. 15 Evolution of flow velocity in nozzle (upper two cross section shows nozzle exit distributions).

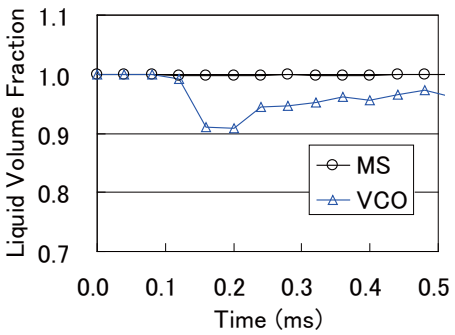

Fig. 16 Liquid volume fraction at nozzle exit.

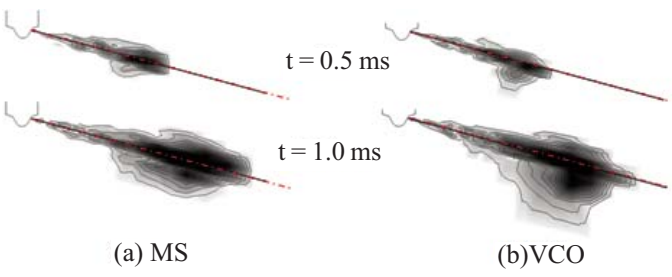

Fig. 17 Liquid mass distribution in the symmetric cross section. (D = 0.14, L = 1.0)

spray is also affected as shown in **Fig. 18**. The vortex position of upper and lower-side is different. And the vorticity distribution is also asymmetric in the VCO nozzle and stronger than of the corresponding MS nozzle. This means downward flow is induced in the spray, and the spray direction deviation could be kept. It is worthwhile to note that this feature of VCO nozzle minimizes with increasing the nozzle L/D, but it even appears in a MS nozzle depending on the nozzle design specification.

There are some other publications which show an increased deviation towards the side where most cavitation in the nozzle occurs.[14,15] The micro spray angles, that is spray cone angles close to nozzle exit, look similar in the MS and VCO nozzles. The one-sided deviation of the micro spray angle of VCO nozzle is not clear both in the calculation and experiment. Possibly this sensitivity highly depends on the each nozzle type, geometry specification and injection conditions. It is also not clear whether cavitation itself or internal nozzle flow pattern which is induced by cavitation is directly effective. However, the lopsided flow pattern regardless whether cavitating or not seems to be essential on the aspect of the influence on macroscopic spray characteristics.

4. Conclusions

A CFD model to predict Diesel spray characteristics without any specific experimental data for standard injector nozzle geometry has been developed. The model is based on a series calculation methodology linking the three-dimensional Eulerian multiphase nozzle internal flow calculation with the Eulerian-Lagrangian spray calculation. The secondary breakup model is significantly improved to realize it. The calculations from the nozzle internal flow to spray formation in a constant volume vessel are performed for mini-sac and VCO nozzles in common rail injector system. The validation of the calculation results is done by comparison with the measurement data on injection volume flow rate, spray tip penetration, spray angle, SMD and droplet size distributions. It is shown that the present model is applicable to analysis and evaluation of the relations between spray characteristics and the nozzle geometry such as nozzle diameter and length.

From the analysis of calculation results, the following results including relations between spray characteristics and the nozzle geometry are obtained:

- The cavitation in a VCO nozzle tends to be more pronounced than in a MS nozzle.
- Increasing nozzle L/D, the cavitation at nozzle exit is decreasing for both nozzles.
- Even in the MS and VCO nozzles having about the same spray characteristics, which are spray tip penetration, SMD and bottom view image, both of the side view image are different. While the spray shape of MS nozzle is almost symmetric along the injection axis, the one of VCO nozzle is asymmetric. The spray of VCO nozzle grows downside until about 1 ms and it looks spray slightly deviating from the injection axis. This is caused by the initial flow pattern into the nozzle hole and the succeeding cavitation onset keeps the feature.

These results show the nozzle geometry effect on non-evaporating spray characteristics. It may sound like minor differences, but they greatly impact on achieving lowest engine emissions.

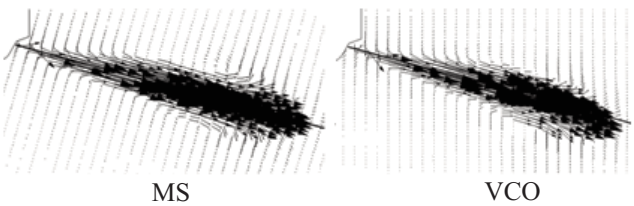

Fig.18 Gas velocity vectors with spray axis. (t = 0.5 ms, D = 0.14, L = 1.0)

Acknowledgment

The authors would like to thank Professor J. Senda of Doushisha Unversity, Dr. I. Sakata of TOYOTA Motor Corporation for providing the experimental data of spray in the constant volume vessels.

References

(1) Soteriu, C., Andrews, R. and Smith, M., "Direct Injection Diesel Sprays and the Effect of Cavitation and Hydraulic Flip on Atomization", *SAE Tech. Pap. Ser.,* No.950080 (1995).
(2) Arcoumanis, C. and Gavaises, M., "Linking Nozzle Flow with Spray Characteristics in a Diesel Fuel Injection System", *Atomization and Sprays*, Vol.8 (1998), pp.307-347.
(3) Han, J., Lu, P., Xie, X., Lai, M. and Henein, N. A., "Investigation of Diesel Spray Primary Break-up and Development for Different Nozzle Geometries", *SAE Tech. Pap. Ser*., No.2002-01-2775 (2002).
(4) Suzzi, D., Kruger, C., Blessing, M., Wenzel, P. and

Welgand, B., "Validation of Eulerian Spray Concept Coupled with CFD Combustion Analysis", *SAE Tech. Pap. Ser*., No.2007-24-0044 (2007).
(5) Masuda, R., Fuyuto, T., Nagaoka, M., von Berg, E. and Tatschl, R., "Validation of Diesel Fuel Spray and Mixture Formation from Nozzle Internal Flow Calculation", *SAE Tech. Pap. Ser*., No.2005-01-2098 (2005).
(6) Tatschl, R., von Künsberg, Sarre, C., Alajbegovic, A. and Winklhofer, E., "Diesel Spray Modelling Including Multidimensional Cavitating Nozzle Flow Effects", *Proc. ILASS-Europe 2000*.
(7) Alajbegovic, A., "Three-Dimensional Cavitation Calculations in Nozzles", *Proc. 2nd Annual Meeting Institute for Multifluid Science and Technology* (1999).
(8) Patterson, M. A. and Reitz, R. D., "Modeling the Effects of Fuel Spray Characteristics on Diesel Engine Combustion and Emission", *SAE Tech. Pap. Ser*., No.980131 (1998).
(9) Nagaoka, M. and Kawamura, K., "A Deforming Droplet Model for Fuel Spray in Direct-Injection Gasoline Engines", *SAE Tech. Pap. Ser*., No.2001-01-1225 (2001).
(10) O'Rourke, P. J. and Amsden, A. A., "The Tab Method for Numerical Calculation of Spray Droplet Breakup", *SAE Tech. Pap. Ser*., No.872089 (1987).
(11) Reitz, R. D., "Modeling Atomization Process in High Pressure Vaporizing Sprays", *Atomization and Spray Tech.*, Vol.3 (1989), pp.309-337.
(12) O'Rourke, P. J. and Bracco, F. V., " Modeling of Drop Interactions in Thick Sprays and a Comparison with Experiments", *IMechE*, C404/80 (1980), pp.101-116.
(13) Schmidt, D. P. and Rutland, C. J., "A New Droplet Collision Algorithm", *Journal of Computational Physics*, Vol.164 (2000), pp.62-80.
(14) Blessing, M., Koenig, G., Krueger, C., Michels, U. and Schwarz, V., "Analysis of Flow and Cavitation Phenomena in Diesel Injection Nozzles and its Effects on Spray and Mixture Formation", *SAE Tech. Pap. Ser*., No.2003-01-1358 (2003).
(15) von Berg, E., Edelbauer, W., Alajbegovic, A. and Tatschl, R., "Coupled Calculation of Cavitating Nozzle Flow, Primary Diesel Fuel Break-up and Spray Formation with an Eulerian Multi-fluid-model", *ICLASS*, 2003 Sorrento, Italy (2003).

Makoto Nagaoka
Research Fields :
- Computational fluid dynamics
- Multi-physics CAE
- Internal combustion engine
- Secondary battery

Academic Degree : Dr. Eng.
Academic Societies :
- Society of Automotive Engineers of Japan
- The Japan Society of Mechanical Engineers
- Institute for Liquid Atomization and Spray Systems-Japan

Awards :
- Paper Award, Japan Society of Automotive Engineers, 1992
- SAE Arch T. Colwell Merit Award, 1996
- Incentive Award, Japan Society of Mechanical Engineers, 1997

Reiko Ueda
Research Fields :
- Computational fluid dynamics
- Fuel injection
- Spray and atomization

Ryo Masuda
Research Fields :
- Computational fluid dynamics
- Fuel injection
- Spray and atomization
- Engine simulation

Academic Societies :
- The Japan Society of Mechanical Engineers
- Society of Automotive Engineers of Japan

Award :
- ILASS-Japan Excellence in Oral Presentation Award, 2002

Eberhard von Berg*
Research Field :
- Spray and mixture formation in IC engines

Reinhard Tatschl*
Research Fields :
- Computational fuid dynamics
- Modeling
- Spray and combustion
- Multi-Physics

Academic Degree : Dipl.-Ing. Dr.

*AVL List GmbH

